

**Electronic Supporting Information**  
**Manuscript ID NJ-ART-04-2019-001774**

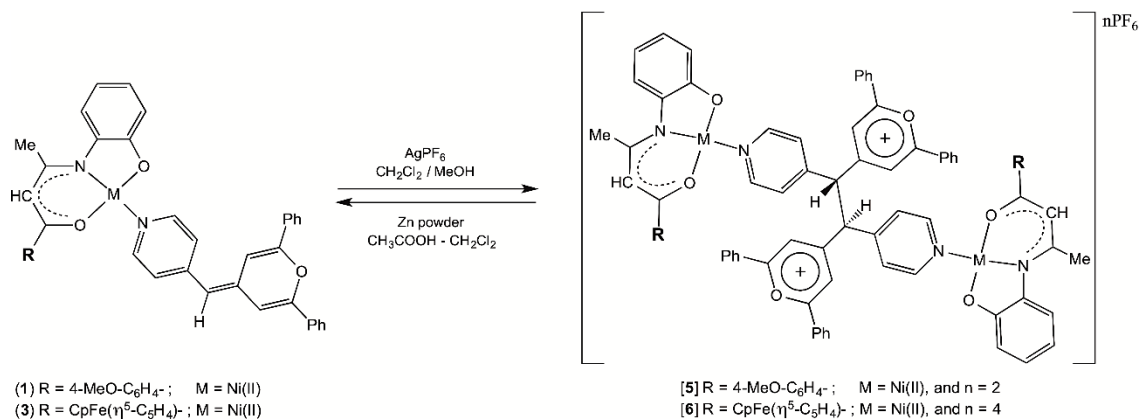
**Redox-Switching of ternary Ni(II) and Cu(II) complexes: Synthesis, experimental and theoretical studies along with second-order nonlinear optical properties**

**Néstor Novoa, Carolina Manzur, Thierry Roisnel, Vincent Dorcet, Nolwenn Cabon, Françoise Robin-Le Guen, Isabelle Ledoux-Rak, Samia Khalal, Jean-Yves Saillard, David Carrillo and Jean-René Hamon**

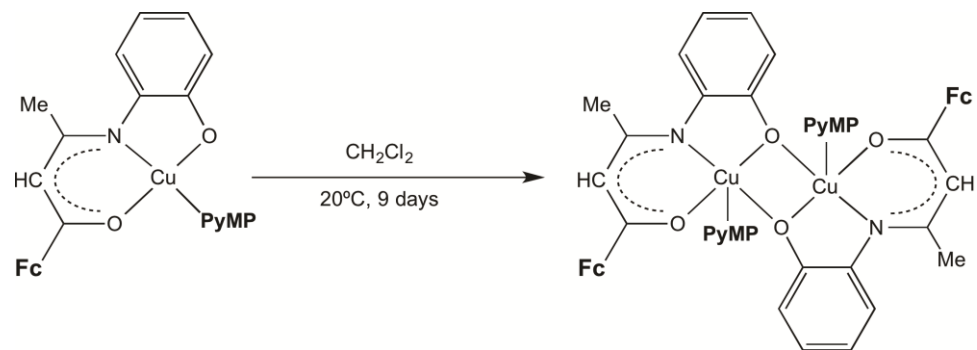
---

**Contents**

<b>Scheme S1.</b> Synthetic procedure to generate compounds <b>5</b> and <b>6</b> .	2
<b>Scheme S2.</b> Formation of the heterotetrametallic complex <b>4'</b> .	2
<b>Chart S1.</b> Hydrogen and carbon atom labeling schemes for <b>1</b> (left) and <b>3</b> (right) used for $^1\text{H}$ NMR assignments.	2
<b>Fig. S1</b> Molecular structure of the Cu(II) mononuclear complex <b>2</b> with the atom labelling scheme. Hydrogen atoms have been omitted for clarity. Thermal ellipsoids are drawn at 50% probability.	3
<b>Fig. S2</b> Cyclic voltammogram of compound <b>2</b> (0.9 mM) in $\text{CH}_2\text{Cl}_2/[n\text{-Bu}_4\text{N}][\text{PF}_6]$ (0.1 M), $v= 0.1 \text{ Vs}^{-1}$ , Pt disk working electrode.	3
<b>Fig. S3</b> Cyclic voltammogram of compound <b>3</b> (0.9 mM) in $\text{CH}_2\text{Cl}_2/[n\text{-Bu}_4\text{N}][\text{PF}_6]$ (0.1 M), $v= 0.1 \text{ Vs}^{-1}$ , Pt disk working electrode.	3
<b>Fig. S4</b> Cyclic voltammogram of compound <b>4</b> (1.1 mM) in $\text{CH}_2\text{Cl}_2/[n\text{-Bu}_4\text{N}][\text{PF}_6]$ (0.1 M), $v= 0.1 \text{ Vs}^{-1}$ , Pt disk working electrode.	4
<b>Fig. S5 A)</b> TLCV of compound <b>3</b> (1 mM) in $\text{CH}_2\text{Cl}_2/[n\text{-Bu}_4\text{N}][\text{PF}_6]$ (0.1 M), $v= 5 \text{ mV s}^{-1}$ , Pt disk, and <b>B)</b> Evolution of the UV-visible spectrum of compound <b>3</b> during its complete oxidation during the TLCV.	4
<b>Fig. S6</b> Experimental UV-vis spectra of complexes <b>2</b> (top), <b>3</b> (middle) and <b>4</b> (bottom), recorded in $\text{CH}_2\text{Cl}_2$ solutions at 20 °C.	5
<b>Fig. S7</b> Kohn-Sham orbital diagrams of <b>2</b> and <b>4</b> .	6
<b>Table S1.</b> Selected X-ray and corresponding DFT-optimized (into square brackets) bond distances ( $\text{\AA}$ ) and angles ( $^\circ$ ) for compounds <b>1</b> and <b>2</b> .	7
<b>Table S2.</b> Selected X-ray and corresponding DFT-optimized (into square brackets) bond distances ( $\text{\AA}$ ) and angles ( $^\circ$ ) for compounds <b>3</b> and <b>4'</b> .	8
<b>Table S3.</b> Metrical parameters of the ferrocenyl units in compounds <b>3</b> and <b>4'</b> .	8



**Scheme S1.** Synthetic procedure to generate compounds **5** and **6**.



**Scheme S2.** Formation of the heterotetrametallic complex **4'**.

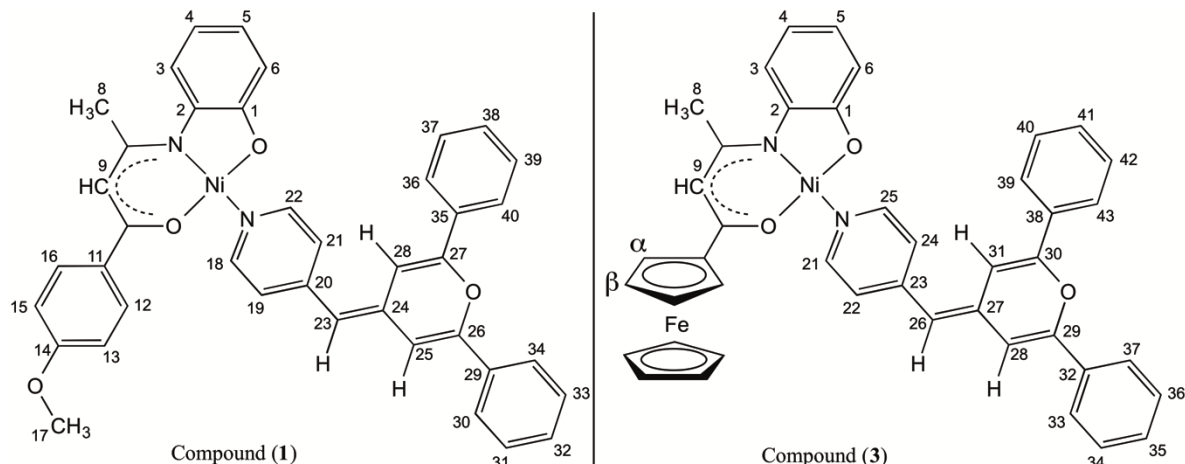


**Chart S1.** Hydrogen and carbon atom labeling schemes for **1** (left) and **3** (right) used for <sup>1</sup>H NMR assignments.

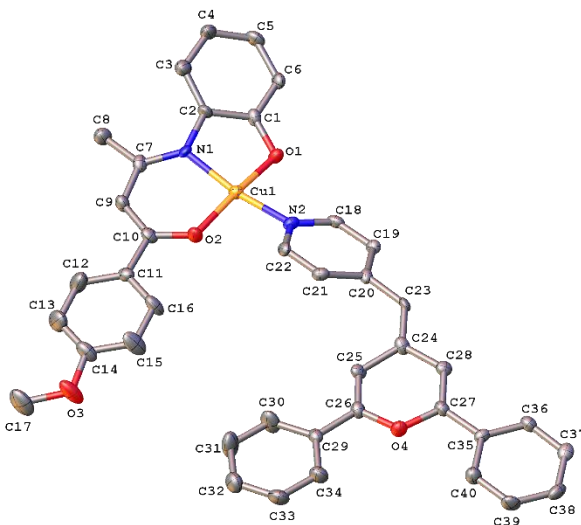


**Fig. S1** Molecular structure of the Cu(II) mononuclear complex **2** with the atom labelling scheme. Hydrogen atoms have been omitted for clarity. Thermal ellipsoids are drawn at 50% probability.

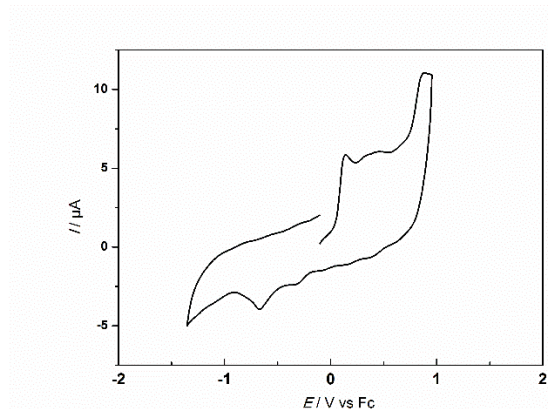


**Fig. S2** Cyclic voltammogram of compound **2** (0.9 mM) in  $\text{CH}_2\text{Cl}_2/[n\text{-Bu}_4\text{N}][\text{PF}_6]$  (0.1 M),  $v=0.1 \text{ Vs}^{-1}$ , Pt disk working electrode.

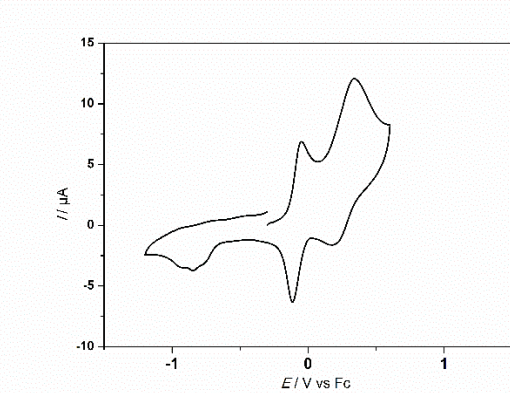


**Fig. S3** Cyclic voltammogram of compound **3** (0.9 mM) in  $\text{CH}_2\text{Cl}_2/[n\text{-Bu}_4\text{N}][\text{PF}_6]$  (0.1 M),  $v=0.1 \text{ Vs}^{-1}$ , Pt disk working electrode.

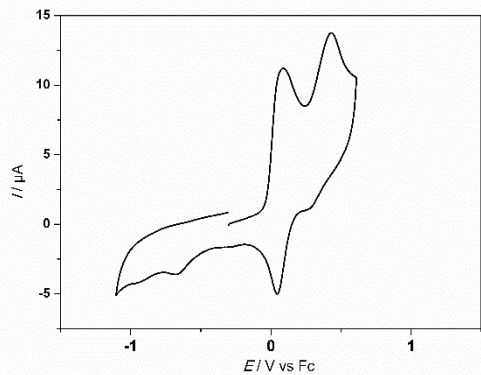


**Fig. S4** Cyclic voltammogram of compound **4** (1.1 mM) in  $\text{CH}_2\text{Cl}_2/[n\text{-Bu}_4\text{N}][\text{PF}_6]$  (0.1 M),  $v=0.1 \text{ Vs}^{-1}$ , Pt disk working electrode.

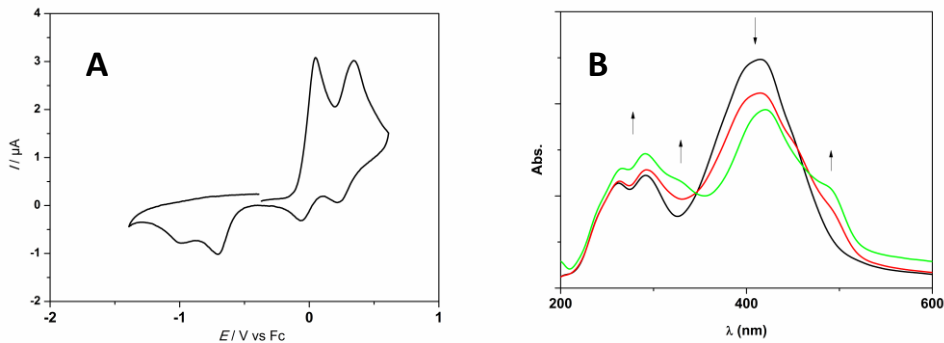


**Fig. S5** **A)** TCV of compound **3** (1 mM) in  $\text{CH}_2\text{Cl}_2/[n\text{-Bu}_4\text{N}][\text{PF}_6]$  (0.1 M),  $v= 5 \text{ mV s}^{-1}$ , Pt disk, and **B)** Evolution of the UV-visible spectrum of compound **3** during its complete oxidation during the TCV.

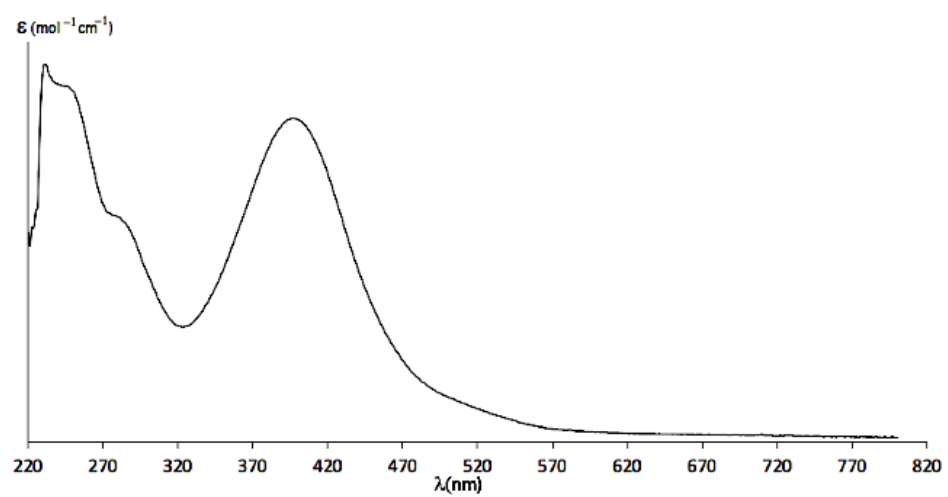
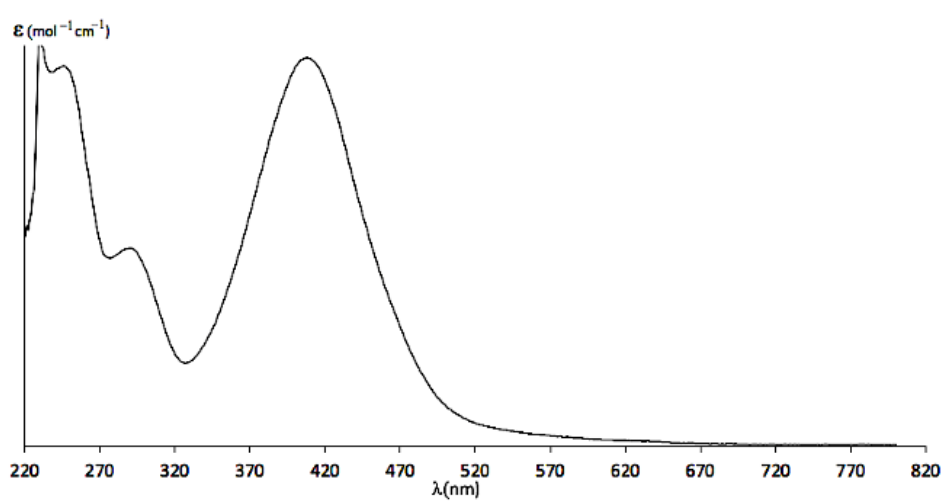
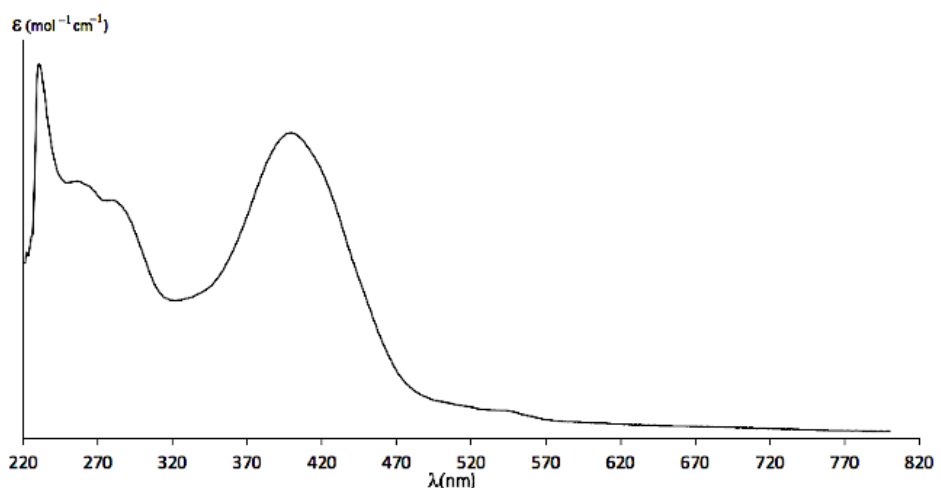


**Fig. S6** Experimental UV-vis spectra of complexes **2** (top), **3** (middle) and **4** (bottom), recorded in CH<sub>2</sub>Cl<sub>2</sub> solutions at 20 °C.

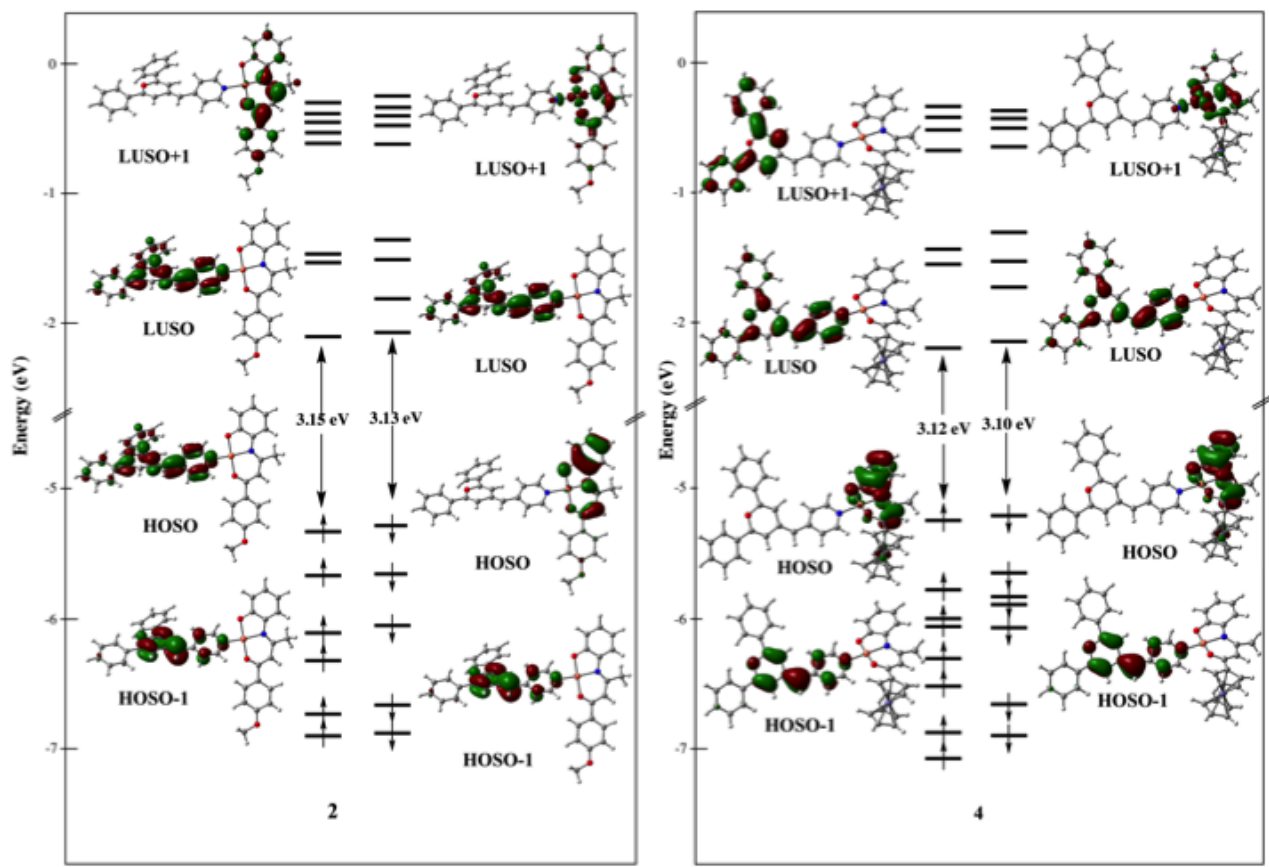


**Fig. S7** Kohn-Sham orbital diagrams of **2** and **4**.

**Table S1.** Selected X-ray and corresponding DFT-optimized (into square brackets) bond distances ( $\text{\AA}$ ) and angles ( $^\circ$ ) for compounds **1** and **2**.

	<b>1</b>	<b>2</b>
Bond distances		
O(1)-C(1)	1.328(3) [1.317]	1.314(8) [1.315]
C(1)-C(2)	1.416(3) [1.413]	1.420(11) [1.420]
N(1)-C(2)	1.420(3) [1.408]	1.419(8) [1.403]
N(1)-C(7)	1.333(3) [1.321]	1.312(8) [1.318]
C(7)-C(9)	1.409(4) [1.409]	1.424(9) [1.413]
C(9)-C(10)	1.372(3) [1.385]	1.392(9) [1.388]
C(10)-O(2)	1.307(3) [1.283]	1.286(8) [1.283]
C(14)-O(3)	1.365(3) [1.349]	1.378(8) [1.343]
C(17)-O(3)	1.419(3) [1.416]	1.428(10) [1.416]
N(2)-C(18)	1.348(3) [1.338]	1.341(9) [1.339]
N(2)-C(22)	1.342(3) [1.341]	1.360(8) [1.341]
C(23)-C(24)	1.364(3) [1.371]	1.377(8) [1.372]
C(25)-C(26)	1.331(3)	1.342(8)
C(27)-C(28)	1.347(4)	1.353(8)
C(26)-O(4)	1.384(3) [1.359]	1.373(8) [1.358]
C(27)-O(4)	1.377(3) [1.353]	1.379(8) [1.353]
Bond angles		
M(1)-O(1)-C(1)	112.18(15) [111.9]	110.7(4) [111.3]
M(1)-N(1)-C(2)	110.39(16) [110.2]	108.5(5) [109.8]
M(1)-N(1)-C(7)	123.82(18) [123.4]	124.4(5) [122.6]
M(1)-O(2)-C(10)	125.83(16) [125.7]	125.9(4) [124.5]
M(1)-N(2)-C(18)	122.42(16) [121.0]	123.7(5) [120.6]
M(1)-N(2)-C(22)	120.87(17) [121.6]	119.6(5) [122.1]
N(1)-C(7)-C(9)	122.4(2) [122.3]	122.4(7) [122.4]
C(7)-C(9)-C(10)	126.2(3) [125.8]	125.9(7) [127.2]
C(9)-C(10)-O(2)	123.7(2) [124.0]	125.1(6) [124.8]
C(14)-O(3)-C(17)	117.1(2) [118.1]	117.3(6) [118.2]
C(20)-C(23)-C(24)	132.4(2) [131.1]	128.2(7) [130.6]
C(23)-C(24)-C(25)	118.6(2) [118.9]	124.6(7) [119.0]
C(23)-C(24)-C(28)	128.4(2) [127.4]	121.7(7) [127.3]
C(26)-O(4)-C(27)	117.81(18) [119.6]	119.7(5) [119.7]

**Table S2.** Selected X-ray and corresponding DFT-optimized (into square brackets) bond distances ( $\text{\AA}$ ) and angles ( $^\circ$ ) for compounds **3** and **4'**.

	<b>3</b>	<b>4'</b>
Bond distances		
O(1)-C(1)	1.335(3) [1.317]	1.339(3)
C(1)-C(2)	1.412(4) [1.413]	1.430(4)
N(1)-C(2)	1.430(3) [1.408]	1.419(4)
N(1)-C(7)	1.331(3) [1.322]	1.323(4)
C(7)-C(9)	1.407(4) [1.407]	1.414(4)
C(9)-C(10)	1.377(3) [1.385]	1.385(4)
C(10)-O(2)	1.298(3) [1.283]	1.299(4)
N(2)-C(21)	1.353(3) [1.341]	1.329(4)
N(2)-C(25)	1.345(3) [1.338]	1.342(4)
C(26)-C(27)	1.365(3) [1.371]	1.364(4)
C(28)-C(29)	1.334(3)	1.334(4)
C(30)-C(31)	1.344(3)	1.330(4)
C(29)-O(3)	1.380(3) [1.354]	1.378(4)
C(30)-O <sub>3</sub>	1.382(3) [1.359]	1.381(4)
Fe(1)-C(Cp)	2.044(3) [2.050]	2.047(3)
Fe(1)-C(Cp')	2.045(3) [2.050]	2.047(3)
Bond angles		
M(1)-O(1)-C(1)	112.03(16) [111.99]	111.77(19)
M(1)-N(1)-C(2)	109.97(16) [110.20]	110.31(19)
M(1)-N(1)-C(7)	123.68(18) [123.32]	122.3(2)
M(1)-O(2)-C(10)	125.67(17) [125.17]	122.03(19)
M(1)-N(2)-C(21)	121.31(17) [121.24]	119.5(2)
M(1)-N(2)-C(25)	121.77(17) [121.36]	122.2(2)
N(1)-C(7)-C(9)	122.2(2) [122.15]	121.3(3)
C(7)-C(9)-C(10)	126.4(2) [125.74]	128.9(3)
C(9)-C(10)-O(2)	124.3(2) [124.38]	125.7(3)
C(26)-C(27)-C(28)	131.9(2) [119.02]	120.8(3)
C(26)-C(27)-C(31)	127.9(2) [127.30]	126.4(3)
C(29)-O(3)-C(30)	118.59(19) [119.62]	117.9(2)

**Table S3.** Metrical parameters of the ferrocenyl units in compounds **3** and **4'**.

Compd	Fe-Cp <sub>CNT</sub> ( $\text{\AA}$ )	Fe-Cp' <sub>CNT</sub> ( $\text{\AA}$ )	Cp <sub>CNT</sub> -Fe-Cp' <sub>CNT</sub> ( $^\circ$ )	Cp/Cp' ( $^\circ$ )
<b>3</b>	1.651	1.652	178.98	8.08
<b>4'</b>	1.650	1.652	179.64	1.98

Abbreviations: Cp = C<sub>5</sub>H<sub>5</sub>, Cp' = C<sub>5</sub>H<sub>4</sub>, CNT = centroid.